APPLIED AND ENVIRONMENTAL MICROBIOLOGY, Apr. 2009, p. 2099–2110 Vol. 75, No. 7
0099-2240/09/$08.00+0 doi:10.1128/AEM.02066-08

Codon-Optimized Fluorescent Proteins Designed for Expression in Low-GC Gram-Positive Bacteria[▽]

Inka Sastalla, Kannie Chim, Gordon Y. C. Cheung, Andrei P. Pomerantsev, and Stephen H. Leppla*

Laboratory of Bacterial Diseases, National Institute of Allergy and Infectious Diseases, National Institutes of Health, Bethesda, Maryland 20892-3202

Received 5 September 2008/Accepted 13 January 2009

Fluorescent proteins have wide applications in biology. However, not all of these proteins are properly expressed in bacteria, especially if the codon usage and genomic GC content of the host organism are not ideal for high expression. In this study, we analyzed the DNA sequences of multiple fluorescent protein genes with respect to codons and GC content and compared them to a low-GC gram-positive bacterium, *Bacillus anthracis*. We found high discrepancies for cyan fluorescent protein (CFP), yellow fluorescent protein (YFP), and the photoactivatable green fluorescent protein (PAGFP), but not GFP, with regard to GC content and codon usage. Concomitantly, when the proteins were expressed in *B. anthracis*, CFP- and YFP-derived fluorescence was undetectable microscopically, a phenomenon caused not by lack of gene transcription or degradation of the proteins but by lack of protein expression. To improve expression in bacteria with low genomic GC contents, we synthesized a codon-optimized *gfp* and constructed optimized photoactivatable *pagfp*, *cfp*, and *yfp*, which were in contrast to nonoptimized genes highly expressed in *B. anthracis* and in another low-GC gram-positive bacterium, *Staphylococcus aureus*. Using optimized GFP as a reporter, we were able to monitor the activity of the protective antigen promoter of *B. anthracis* and confirm its dependence on bicarbonate and regulators present on virulence plasmid pXO1.

Fluorescent proteins (FPs) based on the *Aequoria* green FP (GFP) are widely used for elucidating molecular mechanisms in cells and bacteria. Today, a large number of different FPs are available from different groups of cnidaria, some of which exhibit distinct absorption and emission spectra, superior folding, and improved activation at higher temperatures (14, 38, 50). Unlike other fluorescent reporters, the chromophore in the *Aequoria* GFP is intrinsic to the primary protein structure and consequently, in addition to oxygen needed for the activation of the chromophore, does not require substrates or other cofactors to fluoresce (8, 17, 46). FPs have found wide applications not only in eukaryotes but also in prokaryotes, including reporter systems to monitor protein expression or promoter activity or for analysis of protein localization within the cell (48). To elucidate bacterial protein expression, it would be desirable to have multiple fluorescent markers available for expression in the target bacterium; Suel et al. (42), for example, analyzed the regulatory circuit of *Bacillus subtilis* competence using multiple FPs. However, not all FPs are expressed properly in all bacteria. To overcome these problems, Veening and colleagues were able to increase FP expression in *B. subtilis* by 20 to 70% by adding the first eight amino acids of ComGA to the N-terminal sequences of cyan FP (CFP) and yellow FP (YFP), speculating that the overcoming of a slow translation initiation caused by the eukaryotic codon bias led to this expression improvement (49). In addition, codon optimizations have been successfully used to increase expression of extrinsic proteins in different cells (3, 27). Using this method, unfavorable or rare codons in an extrinsic gene are exchanged in favor of more abundant ones without affecting amino acid sequences. This approach not only may lead to higher expression yields of recombinant proteins in bacteria and mammalian cells (3, 27, 34, 43, 51) but may also lead to fewer mistranslations, therefore improving the quality of the protein (22).

Gram-positive bacteria can be divided into two distinct groups: those with an overall high GC content, including *Mycobacteria* and *Streptomyces*, and those with low genomic GC content, such as *Bacillus*, *Lactococcaceae*, and *Clostridia* (28). *Bacillus anthracis*, the causative agent of anthrax, belongs to the latter group. We hypothesized that by replacing rare GC-rich codons with more abundant, AT-rich ones, we could improve gene expression of FPs in a low-genomic-GC-content bacterium such as *B. anthracis*. Our ultimate aims were the acquisition of a variety of colors for investigating molecular mechanisms in these prokaryotes and the improvement of FP expression. Codon optimizations by gene synthesis are widely offered and present a cost-effective way to increase recombinant protein yield.

Here we show that by exchanging amino acids of just one codon-optimized protein, we were able to obtain three FPs: YFPopt, CFPopt, and PAGFPopt, a photoactivatable GFP (31). All FPs, including the codon-optimized GFP, GFPopt, are highly expressed not only in *B. anthracis* but also in *Staphylococcus aureus* and can be used to analyze promoter activity. The corresponding genes have a low GC content and may be suitable for expression in other low-GC gram-positive bacteria.

* Corresponding author. Mailing address: Laboratory of Bacterial Diseases, National Institute of Allergy and Infectious Diseases, National Institutes of Health, Building 33, Bethesda, MD 20892-3202. Phone: (301) 594-2865. Fax: (301) 480-9997. E-mail: sleppla@niaid.nih.gov.

▽ Published ahead of print on 30 January 2009.

MATERIALS AND METHODS

Bacterial strains, media, and growth conditions. All strains used in this study are listed in Table 1. *Escherichia coli* strains used for cloning purposes were grown in Luria-Bertani (LB) broth or plates. *B. anthracis* strain Ames 33, a

TABLE 1. Strains and plasmids used in this study

Plasmid or strain	Relevant characteristic(s)[a]	Source or reference
Strains		
E. coli		
TOP10		Invitrogen
SCS110		Stratagene
B. anthracis		
Ames 33	pXO1$^-$ pXO2$^-$	32
Ames 35	pXO1$^+$ pXO2$^-$	32
A33(pSW4-GFPmut1)	Ames 33 electroporated with pSW4-GFPmut1, Km^r	This study
A33(pSW4-GFPopt)	Ames 33 electroporated with pSW4-GFPopt, Km^r	This study
A33(pSW4-CFP)	Ames 33 electroporated with pSW4-CFP, Km^r	This study
A33(pSW4-CFPopt)	Ames 33 electroporated with pSW4-CFPopt, Km^r	This study
A33(pSW-PAGFPopt)	Ames 33 electroporated with pSW4-PAGFPopt, Km^r	This study
S. aureus		
RN4220	Hemolysin-defective *S. aureus* strain, Sp^r	13
RN(pTetONGFPopt)	RN4220 electroporated with pTetONGFPopt, Sp^r	This study
RN(pTetONCFPopt)	RN4220 electroporated with pTetONCFPopt, Sp^r	This study
RN(pTetONYFPopt)	RN4220 electroporated with pTetONYFPopt, Sp^r	This study
Plasmids		
pCR2.1 TOPO	Cloning vector, Km^r Ap^r	Invitrogen
pUC18-GFPopt	Vector harboring custom codon-optimized GFPmut1, Ap^r	BlueHeron
pS10-CFP	pCR2.1 harboring CFP under the control of S10 promoter of *S. aureus*	This study
pS10-CFPopt	pCR2.1 harboring CFPopt under the control of S10 promoter of *S. aureus*	This study
pSW4	Gram-positive/gram-negative shuttle vector with PA promoter, Km^r Ap^r	32
pSW4-GFPmut1	pSW4 plasmid containing 729-bp AseI/BamHI-cloned *gfpmut*1	This study
pSW4-GFPopt	pSW4 plasmid containing 729-bp AseI/BamHI-cloned *gfpopt*	This study
pSW4-CFP	pSW4 plasmid containing 732-bp AseI/BamHI-cloned *cfp*	This study
pSW4-CFPopt	pSW4 plasmid containing 732-bp AseI/BamHI-cloned *cfpopt*	This study
pSW4-YFP	pSW4 plasmid containing 732-bp AseI/BamHI-cloned *yfp*	This study
pSW4-YFPopt	pSW4 plasmid containing 729-bp AseI/BamHI-cloned *yfpopt*	This study
pSW4-PAGFP	pSW4 plasmid containing 732-bp AseI/BamHI-cloned *pagfp*	This study
pYJ335	Vector with tetracycline-inducible $P_{xyl/tetO}$ promoter	20
pJRS312	Vector containing spectinomycin cassette	36
pTetON	pYJ335 derivative with inactive tetracycline repressor promoter, Ap^r Sp^r	This study
pTetONGFPopt	pTetON containing 729-bp *gfpopt* cloned via SmaI/SbfI	This study
pTetONCFPopt	pTetON containing 729-bp *cfpopt* cloned via SmaI/SbfI	This study
pTetONYFPopt	pTetON containing 729-bp *cfpopt* cloned via SmaI/SbfI	This study

[a] Abbreviations: Ap^r, ampicillin resistance; Km^r, kanamycin resistance; Sp^r, spectinomycin resistance.

pXO1$^-$/pXO2$^-$ derivative of strain Ames 34 (32), and strain Ames 35 (pXO1$^+$/pXO2$^-$) were grown in LB broth or NBY broth, containing 0.8% (wt/vol) nutrient broth, 0.3% yeast extract, 0.5% glucose, 1% fetal bovine serum (FBS), and 0.9% sodium bicarbonate. Bacteria were grown at 37°C and 225 rpm in either air or air supplemented with CO_2 regulated at 5% (vol/vol). Sporulation plates contained 0.92% nutrient broth, 0.001% $MnSO_4$, 0.001% KH_2PO_4, and 1.8% agar. *S. aureus* strain RN4220, a gift from Michael Otto, was grown in tryptic soy broth (TSB) at 37°C and 225 rpm or on tryptic soy agar. When required, the following antibiotics (Sigma) were added: ampicillin (100 μg/ml), kanamycin (20 μg/ml for *B. anthracis* and 100 μg/ml for *S. aureus*), and spectinomycin (100 μg/ml).

Site-directed mutagenesis. *gfpopt* was synthesized by oligonucleotide assembly performed by BlueHeron. For generation of *cfpopt*, *yfpopt*, and *pagfpopt* by site-directed mutagenesis using *gfpopt* as a template, the Stratagene QuikChange Multi Kit was used as recommended by the manufacturer. During the mutagenesis, the following nucleotides were subjected to exchange: (i) for *cfpopt*, A197G, C198G, A437T, T458C, A692T, and C693A (in addition, a GTT coding for a valine at position 2 of the protein was incorporated into *cfpopt*, because this codon is also present in *cfp*); (ii) for *yfpopt*, A193G, C194G, G202C, T214G, A607T, C608A, and G609T; and (iii) for *pagfpopt*, A192T, A193T, T488C, A607C, C608A, and G609T. All oligonucleotides designated with "SDM" (Table 2) were designed using the Stratagene web page (http://stratagene.com/TechToolbox) and were used to amplify the entire pUC18-GFPopt plasmid. PCR was performed as recommended, with an extension time of 6 min 45 s. Template DNA was subsequently digested with DpnI, and the residual plasmids, pUC18-CFPopt, pUC18-YFPopt, and pUC18-PAGFPopt, were transformed into XL10-Gold (Stratagene). Positive transformants were identified by PCR and verified by sequencing using M13 primers.

Recombinant DNA techniques. Vectors pSW4-GFPopt, pSW4-GFPmut1, pSW4-CFP, pSW4-CFPopt, pSW4-YFP, pSW4-YFPopt, and pSW4-PAGFPopt (Table 2) were constructed as follows. Fluorescent genes were amplified with proofreading Phusion polymerase (New England Biolabs) from pUC18 with oligonucleotides FPAsefw and FPBamrv for codon-optimized constructs, CFPfw in combination with CFPrv for *cfp*, and YFPfw in combination with YFPrv for *yfp*, incorporating a BamHI restriction site at the 3′end and an AseI restriction site at the 5′end. Templates for *yfp* and *cfp* amplification were the vectors pIYFP and pICFP, respectively (49), which we received from the *Bacillus* Genetic Stock Center. PCR fragments were subsequently cloned into TOPO pCR2.1 (Invitrogen), and positive TOP10 clones were sequenced with M13 primers to verify the fidelity of the insert. pSW4 was restricted with NdeI and BamHI, and FP genes were ligated into the vector via BamHI and AseI sites; the latter site has single-strand extensions compatible with NdeI products. Positive XL2Blue clones were verified by restriction analysis and sequencing, using oligonucleotide pSW4seq, which anneals in pSW4.

To generate CFP fusions with the S10 promoter of *S. aureus*, the S10 promoter was amplified using oligonucleotide S10fwAse in combination with S10CFPrv with genomic DNA of strain RN4420 as a template. *cfp* was amplified with oligonucleotide CFPSOEfw in combination with CFPBamrv, resulting in an overlap with the S10 promoter at the 5′end of the FP gene, as well as incorporation of a BamHI site at the 3′ end. The S10 promoter and FP gene fragments

TABLE 2. Oligonucleotides used in this study

Primer name	Sequence (5′ to 3′)[a]	Restriction site	Purpose
FPAsefw	**GGATTA**TGTCAAAAGGAGAAGAATTATTTACAG	AseI	Amplification of fluorescent protein genes
FPBamrv	**GGATCC**TTACTTATATAATTCATCCATTCCGTG	BamHI	
GFPAsefw	**GGATTA**ATGAGTAAAGGAGAAGAACTTTTCACTG	AseI	Amplification of non-codon-optimized *gfpmut1*
GFPBamrv	**GGATCC**TTATTTGTATAGTTCATCCATGCCA	BamHI	
CFPAsefw	**GGATTA**ATGGTGAGCAAGGGCGA	AseI	Amplification of non-codon-optimized *cfp*
CFPBamrv	**GGATCC**TTACTTGTACAGCTCGTCCATG	BamHI	
YFPAsefw	**GGATTA**ATGGTGAGCAAGGGCGAG	AseI	Amplification of non-codon-optimized *yfp*
YFPBamrv	**GGATCC**TTACTTGTACAGCTCGTCCATGC	BamHI	
SDMCFPV2	TATACAAAAAGGAGAACGCATAATGGTTTCAAAAGGAGAAGAATTATTTACAG	None	Site-directed mutagenesis of *cfpopt* to introduce valine-2 (CFPopt)
SDMCFPH-L	TTCGTAACAGCAGCAGGAATTACACTAGGAATGGATGAATTATATAAGTAAG	None	Site-directed mutagenesis of *gfpopt* for exchange H232L (CFPopt)
SDMCFPSY-TW	GGCCCACACTTGTGACTACTTTAACATGGGGAGTACAATGTTTTTC	None	Site-directed mutagenesis of *gfpopt* for exchanges S65T and Y66W (CFPopt)
SDMCFPN-I	GGACATAAATTAGAATACAATTACATCAGTCATAACGTATACATAATGGCA	None	Site-directed mutagenesis of *gfpopt* for exchange N146I (CFPopt)
SDMCFPM-T	AGAATACAATTACAACAGTCATAACGTATACATAACGGCAGATAAACAGAAAAA	None	Site-directed mutagenesis of *gpfopt* for exchange M153T (CFPopt)
SDMYFPSV-GL	ATGGCCCACACTTGTGACTACTTTAGGATACGGACTACAATGTTTTTCAAGATATC	None	Site-directed mutagenesis of *gfpopt* for exchanges S65G and V68L (YFPopt)
SDMYFPS-A	TTTAACATACGGAGTACAATGTTTTGCAAGATATCCAGATCATATGAAAC	None	Site-directed mutagenesis of *gfpopt* for exchange S72A (YFPopt)
SDMYFPT-Y	CTTCTACCAGATAATCATTACTTAAGCTATCAAAGCGCTTTATCTAAAGACCCAAA	None	Site-directed mutagenesis of *gfpopt* for exchange T203Y (YFPopt)
SDMPAGFPLT-FS	GGCCCACACTTGTGACTACTTTTTCATACGGAGTACAATGTTTTTC	None	Site-directed mutagenesis of *gfpopt* for exchanges L64F and T65S (PAGFPopt)
SDMPAGFPS-A	GGCAGATAAACAGAAAAATGGAATTAAAGCTAACTTTAAAATAAGACACAATATAGAAG	None	Site-directed mutagenesis of *gfpopt* for exchange V163A (PAGFPopt)
SDMPAGFPT-H	CTTCTACCAGATAATCATTACTTAAGCCATCAAAGCGCTTTATCTAAAGACCCAAA	None	Site-directed mutagenesis of *gfpopt* for exchange T203H (PAGFPopt)
pSW4Seq	AAAGTTCTGTTTAAAAAGCCAAAAAT	None	Sequencing oligonucleotide for verification of pSW4 inserts
M13f	GTAAAACGACGGCCAGT	None	Sequencing oligonucleotide for verification of pCR2.1 inserts
M13r	AACAGCTATGACCATG	None	Sequencing oligonucleotide for verification of pCR2.1 inserts
S10fwAse	**GGATTA**ATATTCACCACCGTTCTTATGACTA	AseI	Forward primer to amplify S10 promoter from *S. aureus*
S10CFPrv	*CTTGCTCACCAT*AATTTTCCCTCCTTATTCGTCTA	None	Reverse primer for S10 promoter with *cfp* overlap
S10CFPoptrv	*CTTTTGAAACCAT*AATTTTCCCTCCTTATTCGTCTA	None	Reverse primer for S10 promoter with *cfpopt* overlap
CFPoptBclfw	AT**TGATCA**TACAAAAAGGAGAACGCATAATGGTGAGCAAGGGCGA	BclI	Amplification of *cfpopt* with ribosomal binding site for pTetON cloning
CFPoptBamrv	G**GATCC**TTACTTATATAATTCATCCATTCCTAGTG	BamHI	

Continued on following page

TABLE 2—*Continued*

Primer name	Sequence (5′ to 3′)[a]	Restriction site	Purpose
YFPoptBclfw	AT**TGATCA**TACAAAAAGGAGAACGCATAATGTCAAAAGGAGAAGA ATTATTTACAG	BclI	Amplification of *yfpopt* with ribosomal binding site for
YFPoptBamrv	CG**GGATCC**TTACTTATATAATTCATCCATTCCGTG	BamHI	pTetON cloning
CFPSOEfw	*GGAGGGAAAATT*ATGGTGAGCAAGGGCGA	None	Forward primer for *cfp* with S10 promoter overlap
CFPoptSOEfw	*GGAGGGAAAATT*ATGGTTTCAAAAGGAGAAGAATT	None	Forward primer for *cfpopt* with S10 promoter overlap
GyrAfw	AAAACCTGTGCATCGTAGGG	None	Forward primer for *gyrA*
GyrArv	ACATTAGCATTGGCATCACG	None	Reverse primer for *gyrA*

[a] Restriction sites are in boldface, and overlaps are in italic.

were fused by overlap extension PCR (18) and cloned into pCR2.1 (Invitrogen), and single colonies were directly analyzed for CFP fluorescence by microscopy.

For expression of CFPopt and YFPopt in *S. aureus*, both FP genes were amplified using oligonucleotide CFPoptBclfw in combination with CFPoptBamrv and oligonucleotide YFPoptBclfw with YFPoptBamrv, respectively. After subcloning into pCR2.1 (Invitrogen), sequencing to verify the fidelity of the construct, and transformation of plasmids into *E. coli* strain SCS110 to receive nonmethylated DNA, fragments were excised with BclI and BamHI and ligated into vector pTetON, which is a derivative of plasmid pYJ335 (20) to which the following changes have been made: (i) the erythromycin resistance cassette was replaced by a spectinomycin cassette originating from vector pJRS312 (36); (ii) the tetracycline repressor gene was exchanged with an improved repressor called tetR(B/D), which has superior repression characteristics (37); and (iii) the *tetR* promoter was replaced by an *xylA* promoter from *Bacillus megaterium* (21), which is nonfunctional in *S. aureus*, and consequently, in the absence of tetR(B/D), any gene placed under the control of the (normally) tetracycline-inducible promoter will be constitutively expressed. All oligonucleotides used in this study are listed in Table 2.

Transformation and analysis of recombinant bacteria. *B. anthracis* was transformed as described previously (30) and plated onto selective LB agar.

S. aureus competent bacteria were prepared as described by Fitzgerald (15). Briefly, bacteria were grown in 25 ml TSB until an optical density of 1.0 at 600 nm was reached, washed multiple times in 10% glycerol (vol/vol), and resuspended in the same buffer, and then 1 μg of plasmid DNA was added. Bacteria were electroporated at 1.75 kV, 100 Ω, and 25 μF. TSB was added, and the suspension was incubated at 37°C for 1 h before aliquots were plated on tryptic soy agar containing the appropriate antibiotic.

To verify the presence of plasmids, colonies were boiled for 2 min at 96°C in either Tris-EDTA buffer (for *B. anthracis*) or lysis buffer (for *S. aureus*), consisting of 1% Triton X-100, 0.5% Tween 20, 10 mM Tris-HCl (pH 8.0), and 1 mM EDTA (41). Bacterial debris were centrifuged for 1 min at 12,000 × *g*, and supernatants were analyzed by PCR.

Microscopy and fluorimetric assays of bacteria. For microscopic evaluation of fluorescence, bacteria grown overnight were diluted in phosphate-buffered saline (PBS) and directly analyzed by microscopy, using a Nikon Eclipse TE2000U microscope with the appropriate filters for detection of CFP (excitation at 405 ± 10 nm and emission at 430 ± 25 nm) or GFP or YFP (excitation at 470 ± 20 nm and emission at 515 nm). For analysis of spores, bacteria were streaked out on spore agar and incubated over a period of 14 days at room temperature. On several subsequent days, spore suspensions were diluted in water and analyzed microscopically. Pictures were taken with a DXM1200C camera (Nikon) and processed using IrfanView. For imaging photoactivatable GFP, a laser-scanning confocal microscope (LSM-510 Zeiss) with a 63×, 1.4-numerical aperture Plan Apochromat oil objective was used. Imaging and photoactivation of PAGFP were performed with the 488-nm line of an argon ion laser (Lasos). The dichroic mirrors used were 413/488 with the appropriate filters supplied by the manufacturer (Carl Zeiss Microimaging, Inc). Photoactivation of PAGFP was performed using 15 iterations of a 413-nm laser (Coherent Enterprise II) at full power in a rectangular region of interest. Two Z-section images of 1 μm in thickness were collected immediately before photoactivation.

To assess protective antigen (PA) promoter-dependent fluorescence in fluorimetric assays, an overnight culture of *B. anthracis* was diluted 1/100 in fresh NBY broth supplemented with FBS with or without 0.9% sodium bicarbonate and grown at 37°C in air or 5% CO_2. Fluorimetric measurements of bacteria grown to different optical densities were performed in a Victor3 reader (Perkin-Elmer) using a GFP filter set (excitation at 485 nm and emission at 535 nm). Fluorescence intensities were normalized against the nonfluorescent wild type.

Flow cytometry. For fluorescence-activated cell sorter (FACS) analysis, bacteria grown overnight were centrifuged, washed, and resuspended at 1/20 in PBS. Samples were analyzed using a FACS Aria cell sorting system (Becton Dickinson) with a 100-mW, 488-nm coherent sapphire solid state laser for GFP and YFP and a 20-mW coherent violet solid state laser for CFP. The fluorescence intensity of 50,000 ungated events was measured in FL-1 and detected at a 515- to 545-nm range with a fluorescein isothiocyanate filter (GFP/YFP) or at a 430- to 470-nm range with a Pacific Blue filter (CFP). *B. anthracis* strain Ames 33 not carrying FP genes served as negative control. Data were analyzed using FACS Diva (Becton Dickinson).

Western blot and protein analysis. Bacteria were grown in 10 ml LB broth until the mid-logarithmic (Ames 33 expressing different FPs) or stationary (for *pagA* promoter analysis) growth phase. Cultures were centrifuged, washed twice with PBS, and resuspended in 500 μl PBS, and bacteria were lysed in a FastPrep system (MP Biomedical) using the FastProtein kit (MP Biomedical) as recommended by the manufacturer. Lysed suspensions were centrifuged briefly, and concentrations of protein lysates were determined using a bicinchoninic acid protein assay kit (Pierce). Equal amounts of cellular proteins were separated by sodium dodecyl sulfate-polyacrylamide gel electrophoresis on a 4 to 20% Tris-glycine gel and blotted onto a nitrocellulose membrane. FPs were subsequently identified using a rabbit anti-GFP polyclonal antibody (Rockland) as the primary antibody and a polyclonal goat anti-rabbit IR800 conjugate (Rockland) as the secondary antibody. The Western blot was developed on an Odyssey infrared scanner (Licor), and bands were quantified using ImageJ software version 1.40g. Protein alignments were performed with the Lasergene MegAlign program (version 7.1.0) using the Clustal W method.

RNA isolation and reverse transcriptase PCR (RT-PCR). Ten milliliters of mid-logarithmic-phase culture was centrifuged and washed once with PBS, and RNA was isolated using a FastRNA Pro kit (MP Biomedical) as recommended by the manufacturer. RNA was ethanol precipitated and resuspended in 50 to 100 μl diethyl pyrocarbonate-treated water, and concentrations were determined using an ND-100 spectrophotometer (Nanodrop).

For RT-PCR, purified RNA was treated with DNase (Ambion) and screened for absence of contaminating DNA by PCR, and 2.5 μg of DNase-treated RNA was subjected to reverse transcription using the Superscript First Strand kit (Invitrogen). To amplify FP genes, the following oligonucleotides were used: FPAsefw and FPBamrv for codon-optimized genes, YFPAsefw and YFPBamrv for *yfp*, CFPAsefw and CFPBamrv for *cfp*, and GFPAsefw in combination with GFPAserv for *gfpmut1*. As an internal control, reactions were also performed with primers GyrAfw and GyrArv, which were designed to amplify a 819-bp fragment of the gyrase A gene (accession no. YP_016609). All primers are listed in Table 2. As negative control, RNA isolated from the Ames 33 wild-type strain was used. Band intensities were quantified using ImageJ version 1.40g.

Statistical analysis. For statistical analysis of differences in mean fluorescence intensities (MFIs), the unpaired *t* test was performed using GraphPad Prism (5.01).

Nucleotide sequence accession numbers. The DNA sequences of all four codon-optimized FP genes have been submitted to GenBank and are available under

TABLE 3. GC content and unfavorable codons in fluorescent protein genes and endogenous genes

Gene	% GC	Unfavorable codons	
		No./total	%
gfpmut1	38.77	96/239	40.17
cfp	61.94	226/240	94.17
yfp	61.53	213/240	88.75
pagfp	61.53	224/240	94.17
gfpopt	33.19	55/239	23.01
cfpopt	33.47	56/240	23.33
yfpopt	33.19	54/240	22.18
gyrA	33.53	185/824	22.45
pagA	33.38	191/765	24.96
srtA (GBAA0688)	33.05	52/234	22.65
spo0A	37.36	76/265	28.67

accession numbers FJ169508 (*gfpopt*), FJ169509 (*cfpopt*), FJ169510 (*yfpopt*), and FJ169511 (*pagfpopt*).

RESULTS

Sequence analysis of *gfpmut1*, *cfp*, *yfp*, and *pagfp*. In comparison to some other bacteria, such as *Mycobacterium tuberculosis* or *Corynebacterium diphtheriae*, *B. anthracis* has an unusually low GC content of approximately 35% (http://cmr.tigr.org/tigr-scripts/CMR/GenomePage.cgi?org=gba). Consequently, for the expression of proteins derived from heterologous organisms having a higher GC content, a low availability of GC-rich codons in *B. anthracis* could be a limiting factor for protein synthesis and a negative influence on protein expression. In an initial in silico analysis, we considered whether *B. anthracis* could be expected to support expression of the *Aequorea victoria*-derived *gfpmut1* gene (11), the *cfp* and *yfp* genes, encoding CFP and YFP, respectively (14), and the *pagfp* gene, encoding a photoactivatable FP (31). The main difference between the last three genes and *gfpmut1*, beyond the obvious differences in fluorescence excitation and emission spectra, is that *cfp*, *yfp*, and *pagfp* are derivatives of Clontech's *egfp*, a gene with high GC content optimized for expression in mammalian cells. *pagfp* represents a photoactivatable GFP, first described by Patterson and Lippincott-Schwartz (31), that is nonfluorescent unless activated with a 413-nm laser. We analyzed the DNA sequences of all four genes with respect to GC content and percentage of unfavorable codons for expression in *B. anthracis*. A codon was deemed unfavorable if it was at least 50% less frequent than the most commonly used codon for a given amino acid in *B. anthracis*. Additionally, for comparison purposes, four randomly picked genes from *B. anthracis* were subjected to the same analysis: (i) sporulation gene *spo0A*, (ii) gyrase subunit A gene *gyrA*, (iii) PA gene *pagA*, and (iv) sortase A gene *srtA*. The results of this analysis are depicted in Table 3 and show that all nonoptimized FP genes exhibit a higher GC content than endogenous genes of *B. anthracis*. *gfpmut1* has the lowest GC content of all four (39%) and the lowest percentage of unfavorable codons. In contrast, *cfp*, *yfp*, and *pagfp* exhibit a substantially higher GC content than intrinsic *B. anthracis* genes. Concomitantly, the percentages of unfavorable codons for *B. anthracis* are 94% (*cfp*), 89% (*yfp*), and 94% (*pagfp*), values greatly elevated in comparison to those for endogenous genes. In comparison, *B. anthracis* endogenous genes have an overall GC content of 33 to 37% and an unfavorable codon percentage of 22 to 29%. Taken together, these data imply that *pagfp*, *cfp*, and *yfp* are more likely to benefit from codon optimization than is *gfpmut1*.

Generation of codon-optimized *gfpmut1*, *cfp*, and *yfp* for expression in *B. anthracis*. Initially, we designed a *gfpmut1* gene with a lower GC content, hoping that it might show superior expression in *B. anthracis*. Using an in silico approach, we exchanged 110 nucleotides in the *gfpmut1* gene, reducing the total number of unfavorable codons from 40% to 23%, which resembles the percentage in endogenous genes (Table 3). The codon-optimized gene, *gfpopt*, was then synthesized and inserted into pUC18 (BlueHeron). This plasmid served as a PCR template for generation of codon-optimized *cfpopt*, *yfpopt*, and *pagfpopt* as outlined in Materials and Methods. An alignment of all codon-optimized FPs with CFPopt is given in Fig. 1. The translated GFPopt had the following exchanges in comparison to GFPopt: Y66W, N146I, M153T, V163A, and H231L, as well as an additional valine at position 2 of the mature protein (Fig. 1). The last two amino acid changes were incorporated to match the protein sequence of CFPopt exactly to that of the Clontech-derived CFP. Consequently, in comparison to the unmodified *cfp*, a total of 410 nucleotides were exchanged in *cfpopt*, leading to a lowered GC content of 33.5% and a decrease in the percentage of unfavorable codons to 23% (Table 3).

```
GFPopt    -MSKGEELFTGVVPILVELDGDVNGHKFSVSGEGEGDATYGKLTLKFICTTGKLPVPWPTLVTTLTYGVQCFSRYPDHMK 79
PAGFPopt  -MSKGEELFTGVVPILVELDGDVNGHKFSVSGEGEGDATYGKLTLKFICTTGKLPVPWPTLVTTFSYGVQCFSRYPDHMK 79
YFPopt    -MSKGEELFTGVVPILVELDGDVNGHKFSVSGEGEGDATYGKLTLKFICTTGKLPVPWPTLVTTLGYGLQCFARYPDHMK 79
CFPopt    MVSKGEELFTGVVPILVELDGDVNGHKFSVSGEGEGDATYGKLTLKFICTTGKLPVPWPTLVTTLTWGVQCFSRYPDHMK 80

GFPopt    QHDFFKSAMPEGYVQERTIFFKDDGNYKTRAEVKFEGDTLVNRIELKGIDFKEDGNILGHKLEYNYNSHNVYIMADKQKN 159
PAGFPopt  QHDFFKSAMPEGYVQERTIFFKDDGNYKTRAEVKFEGDTLVNRIELKGIDFKEDGNILGHKLEYNYNSHNVYIMADKQKN 159
YFPopt    QHDFFKSAMPEGYVQERTIFFKDDGNYKTRAEVKFEGDTLVNRIELKGIDFKEDGNILGHKLEYNYNSHNVYIMADKQKN 159
CFPopt    QHDFFKSAMPEGYVQERTIFFKDDGNYKTRAEVKFEGDTLVNRIELKGIDFKEDGNILGHKLEYNYISHNVYITADKQKN 160

GFPopt    GIKVNFKIRHNIEDGSVQLADHYQQNTPIGDGPVLLPDNHYLSTQSALSKDPNEKRDHMVLLEFVTAAGITHGMDELYK  238
PAGFPopt  GIKANFKIRHNIEDGSVQLADHYQQNTPIGDGPVLLPDNHYLSHQSALSKDPNEKRDHMVLLEFVTAAGITHGMDELYK  238
YFPopt    GIKVNFKIRHNIEDGSVQLADHYQQNTPIGDGPVLLPDNHYLSYQSALSKDPNEKRDHMVLLEFVTAAGITHGMDELYK. 239
CFPopt    GIKANFKIRHNIEDGSVQLADHYQQNTPIGDGPVLLPDNHYLSTQSALSKDPNEKRDHMVLLEFVTAAGITLGMDELYK. 240
```

FIG. 1. Clustal W sequence alignment of all four codon-optimized FPs. Amino acid changes performed with respect to GFPopt are highlighted in gray.

For generation of YFPopt, we performed the following amino acid exchanges in GFPopt: T65G, V68L, S72A, and T203Y (Fig. 1). Although we incorporated all amino acids crucial for a red-shifted fluorescence, our *yfpopt* is based on *gfpopt*, therefore resulting in an aberrant amino acid sequence that is not identical to that of Clontech's YFP. By codon optimization, we were able to reduce the number of unfavorable codons in *yfpopt* to 22% (Table 3), in comparison to 89% in *yfp*.

To design the photoactivatable PAGFP, we initially converted the enhanced GFPopt, having F64L and S65T exchanges that cause loss of the major 397-nm peak in the GFPmut1 emission spectrum (11), back to the original wild-type GFP. A V163A exchange needed for high expression at 37°C (40) was incorporated, as well as the crucial exchange required for photoactivation, T203H (31) (Fig. 1). As for *yfpopt*, the valine at position 2 of the PAGFP protein was not included in the codon-optimized gene. However, in comparison to the nonoptimized *pagfp*, we were able to lower the GC content from 94% to 22% in *pagfpopt* (Table 3), incorporating 225 nucleotide exchanges with respect to *gfpmut1*.

Cloning and expression of FPs in *B. anthracis*. For evaluating protein expression of the unmodified and codon-optimized FPs, we cloned *gfpmut1*, *gfpopt*, *cfp*, *cfpopt*, *yfpopt*, and *pagfpopt* into the gram-positive/*E. coli* shuttle vector pSW4 (32), a derivative of pSJ115 that allows expression of proteins under the control of the *pagA* promoter of *B. anthracis*. PA of *B. anthracis* is the moiety of the anthrax lethal toxin and edema toxin which binds to the eukaryotic cell membrane, using receptors CMG2 and TEM8 (6, 39). This bacterial protein is highly expressed during vegetative growth of bacteria, and consequently its promoter was a promising choice for expression of extrinsic proteins in *B. anthracis*. Furthermore, it has been previously demonstrated that this plasmid is highly suitable for expression of lethal factor of *B. anthracis* (30) and for the *Bacillus cereus* regulator PlcR in *B. anthracis* (32). We found that when using LB broth, expression occurs even in the absence of bicarbonate. The resulting plasmids pSW4-GFPmut1, etc. (Table 1), were partially sequenced to verify accuracy of the genes and promoter regions and electroporated into *B. anthracis* Ames 33, a strain devoid of both virulence plasmids, pXO1 and pXO2 (32).

We then analyzed positive clones grown in LB broth in the absence of bicarbonate to stationary phase for expression of FPs by microscopy (Fig. 2). FPs that were highly expressed in *B. anthracis* were distributed evenly within the bacterium, as seen by homogenous fluorescence (Fig. 2 A, B, E, and H). No obvious difference between the codon-optimized and the unmodified GFPs could be observed visually, indicating that expression of GFPmut1 is not hampered by a reduced availability of less abundant codons. Microscopic analysis of PAGFP-expressing *B. anthracis* is depicted in Fig. 2J and K. Before photoactivation, very little fluorescence was visible, in contrast to the fluorescence observed after activation. Unfortunately, we did not have an original PAGFP for comparison, and therefore no conclusions can be made with respect to higher fluorescence of our codon-optimized *pagfp*.

The most prominent differences were observed for *cfp* and *yfp* compared to their codon-optimized counterparts. Strikingly, we were unable to detect any fluorescence in bacteria or spores harboring the unmodified *cfp* or *yfp* gene (Fig. 2D and G), and at the same time, bacteria expressing the codon-optimized CFPopt and YFPopt were highly fluorescent (Fig. 2E and H). Although we did not detect any fluorescence for CFP in *B. anthracis*, when fused to the S10 promoter of *S. aureus*, CFP was highly expressed in the higher-GC-content bacterium *E. coli* (data not shown). These observations imply that CFPopt and YFPopt may be superior to the conventional FPs with respect to expression in *B. anthracis*.

Fluorescence was also observed in all *B. anthracis* spores and was preserved for a period of at least 14 days (data not shown), indicating that GFP and its derivatives are stable within the cells throughout sporulation, an observation made previously by Ruthel et al. (35). This fluorescence remained stable after heat treatment of spores at 65°C over a period of 30 min, a protocol used for standard spore preparation protocols to inactivate vegetative bacteria (Fig. 2C, F, and I) (1).

MFIs can be assessed by flow cytometric analysis and show levels of FP expression in single bacteria. MFIs of bacteria grown in air corroborated the results obtained by microscopy. Thus, bacteria expressed both GFPopt and GFPmut1 to a similar high level, with MFIs of 10,948 and 13,243, although expression of GFPmut1 was significantly better ($P = 0.0309$, GFP versus GFPopt; $P < 0.0001$, CFP versus CFPopt; $P = 0.0005$, YFP versus YFPopt). Clear differences were also seen between single bacteria expressing CFP and CFPopt, with MFIs of 1,235 and 2,758, respectively, and, more strikingly, between YFP- and YFPopt-positive bacteria, having MFIs of 787 and 10,224, respectively. All differences were significant ($P < 0.05$). A comparison of MFIs of differently colored FPs could not be performed since different lasers and filters were used for excitation and detection. Observed variances in MFI can be attributed to the near absence of a fluorescent signal in CFP- and YFP-expressing bacteria, as FACS plots show (Fig. 3B). These results are consistent with the observations made by microscopy and confirm the superior expression of codon-optimized CFPopt and YFPopt.

Expression and transcription of FP genes. To test whether low protein expression of *yfp* and *cfp* and higher fluorescence of *gfpmut1* were caused by low production of mRNA, we performed semiquantitative RT-PCR experiments to compare transcription levels of the codon-optimized versus original FP genes. *B. anthracis* harboring plasmid pSW4 with FP genes was grown to mid-logarithmic growth phase in LB broth, allowing expression of genes in the absence of bicarbonate, and RNA was extracted and processed as outlined in Materials and Methods. Figure 4A shows that mRNA quantities of all genes were similar; however, in comparison to the internal gyrase A control, transcription levels of nonoptimized CFP and YFP were slightly lower than for the codon-optimized counterparts. This might explain a weaker expression of these FPs but not a total lack of expression.

Consequently, we also investigated whether the lack of CFP and YFP fluorescence was due to rapid degradation of these FPs in *B. anthracis*. Therefore, we performed Western blot analysis of *B. anthracis* protein lysates and evaluated expression of FPs with a polyclonal GFP antibody. The results depicted in Fig. 4B show that in comparison to CFPopt and YFPopt, the original CFP and YFP were poorly or not at all expressed, and we were unable to detect any degradation.

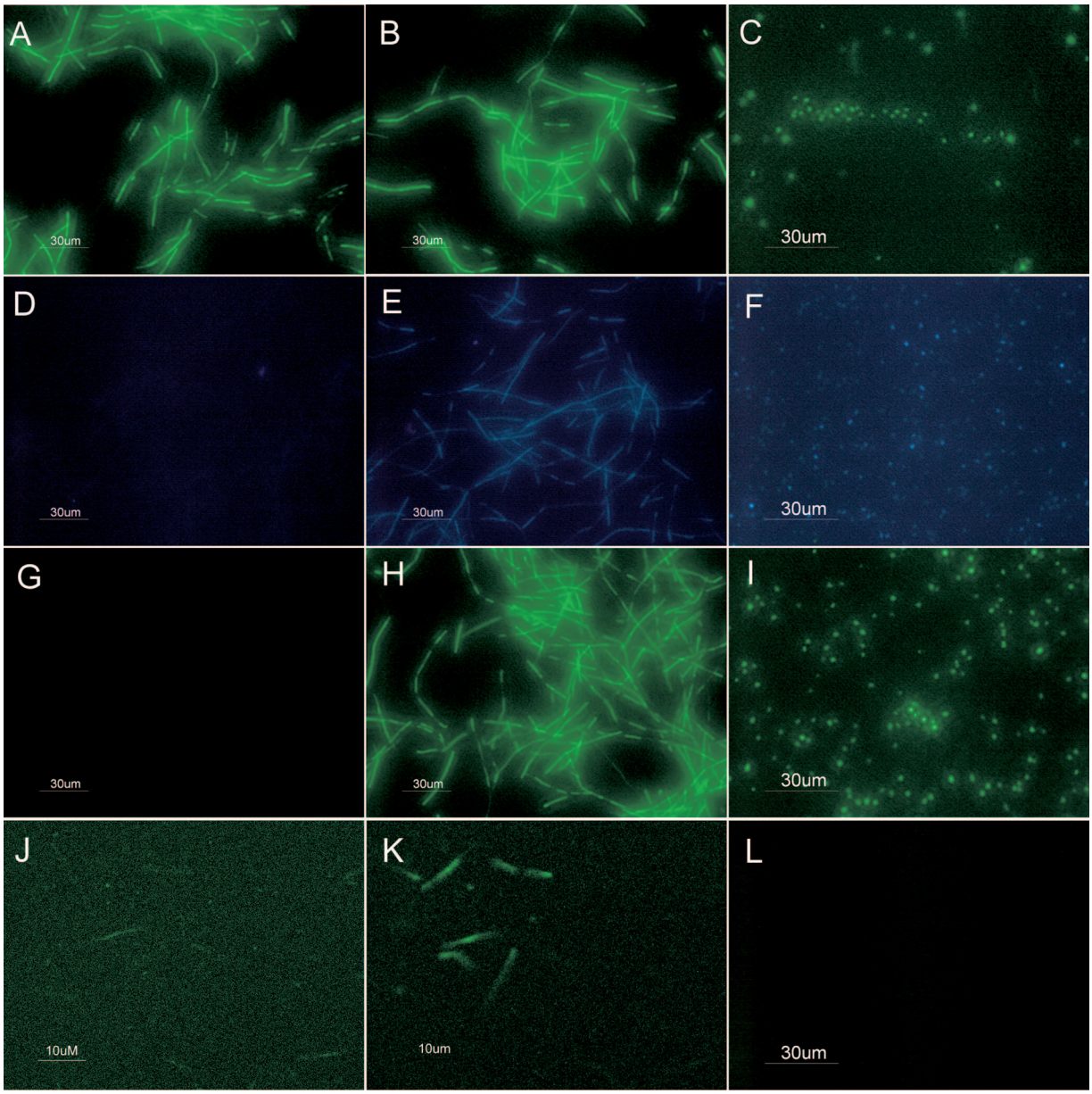

FIG. 2. Visualization of FP production in *B. anthracis* vegetative bacteria and spores by fluorescence microscopy. Strains carrying different FP genes were grown to stationary phase overnight in LB and analyzed by fluorescence microscopy: *B. anthracis* Ames 33 harboring pSW4-GFPmut1 (A), pSW4-GFPopt (B), pSW4-CFP (D), pSW4-CFPopt (E), pSW4-YFP (G), pSW4-YFPopt (H), or pSW4-PAGFP before (J) or after (K) photoactivation with a 413-nm laser. For spore images, bacteria were grown on low-nutrient sporulating plates for multiple days, heat inactivated in order to kill remaining vegetative bacteria, and analyzed by fluorescence microscopy: *B. anthracis* Ames 33 spores expressing GFPopt (C), CFPopt (F), or YFPopt (I) or plasmid-free (L).

Interestingly, even though there was no visible fluorescence when analyzed microscopically and quantitatively, low protein expression was noticeable for CFP.

These results show that the dissimilarities observed in FP expression are unlikely to be caused by differences in mRNA expression or by degradation of FPs but must result from poor expression due to tRNA unavailability. Therefore, although expressed in higher-GC-content bacteria such as *E. coli*, non-codon-optimized YFP and CFP are not suitable for expression in *B. anthracis*.

Analysis of PagA promoter activity using codon-optimized GFPopt. Next, we wanted to test whether our improved codon-optimized FPs are suitable for analysis of promoter activity in *B. anthracis* by analyzing GFPopt production under the control of the *pagA* promoter. In *B. anthracis*, the expression of PA is influenced by two regulators, AtxA and PagR, present on virulence plasmid pXO1, and their activity is determined by the presence of carbon dioxide (12, 24, 47). Whereas AtxA upregulates expression of PA in the presence of CO_2 (24), PagR, which is cotranscribed with PA, negatively influences transcrip-

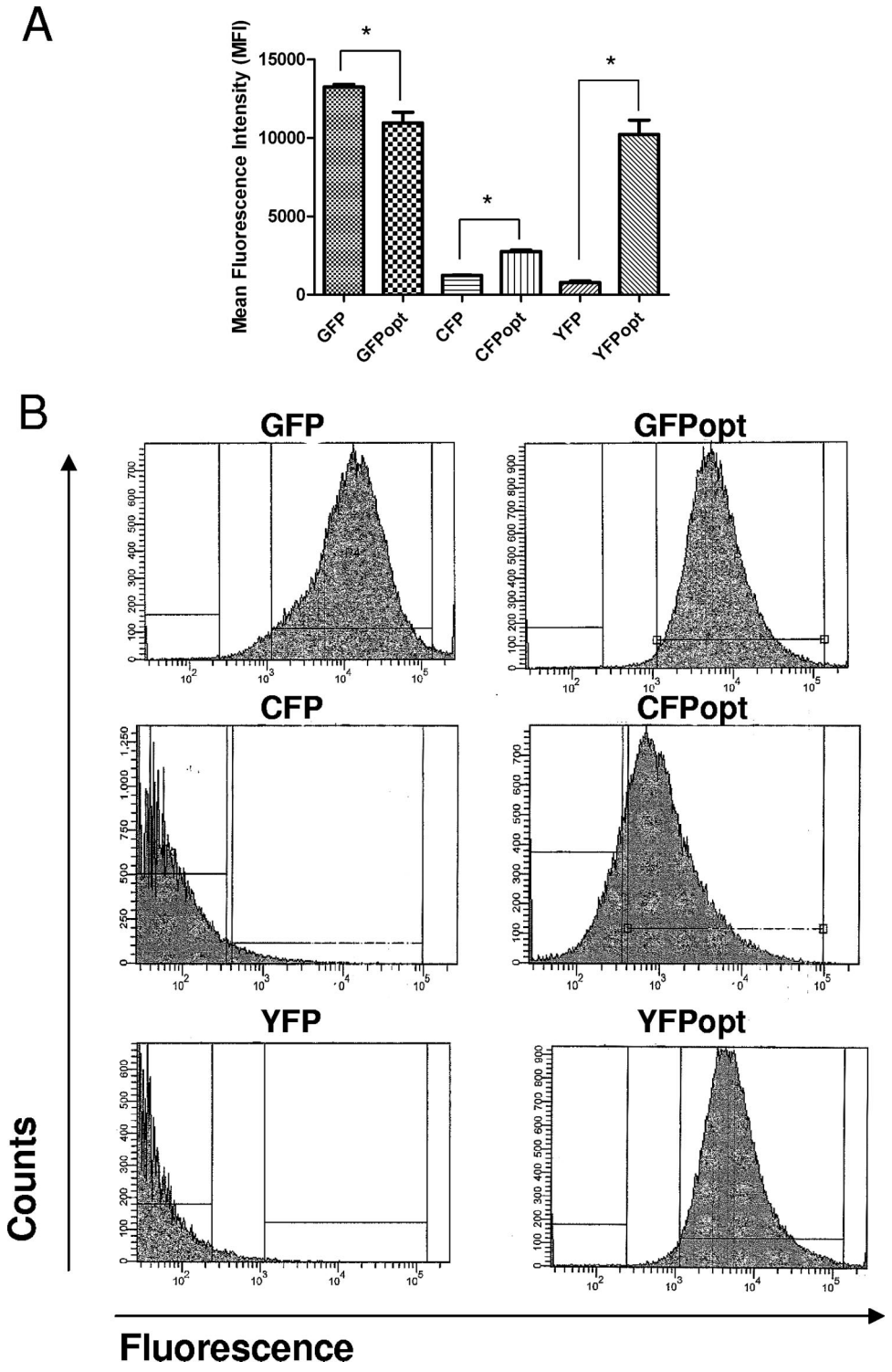

FIG. 3. FACS analysis of bacteria expressing original and codon-optimized FPs. *B. anthracis* Ames 33 carrying pSW4 plasmids with the respective fluorescent genes were grown overnight in LB and subjected to analysis by flow cytometry. (A) Comparison of MFIs of bacteria. All differences were statistically significant ($P = 0.0309$, GFP versus GFPopt; $P < 0.0001$, CFP versus CFPopt; $P = 0.0005$, YFP versus YFPopt). Error bars indicate standard deviations. (B) FACS detection of *B. anthracis* vegetative cells expressing FPs.

tion of *atxA*, therefore causing low PA expression (19). To evaluate whether our optimized FPs are suitable for analysis of promoter activity in *B. anthracis*, we used fluorimetric assays to assess the influence of these factors on *pagA* promoter-driven GFPopt expression. We compared P_{pagA}-dependent GFPopt expression in an AtxA/PagR-harboring strain (Ames 35, pXO1 positive) with that in a regulator-negative strain (Ames 33, pXO1 negative) in the presence and absence of bicarbonate

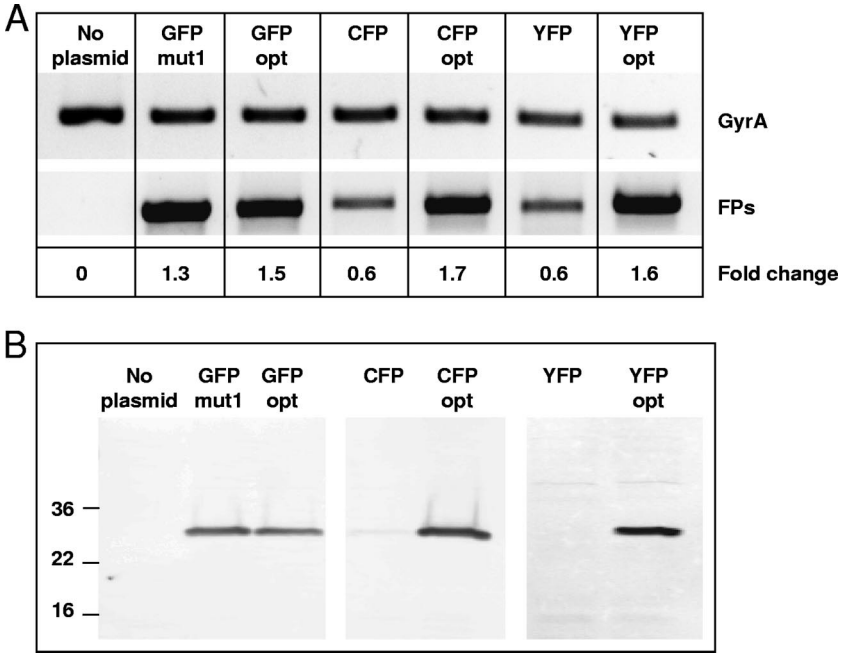

FIG. 4. (A) RT-PCR analysis of mRNA isolated from *B. anthracis* vegetative cells expressing FP genes. *B. anthracis* carrying pSW4 plasmids with FP genes was grown in LB to mid-logarithmic phase, and RNA was extracted as outlined in Materials and Methods. The level of gyrase A (*gyrA*) mRNA served as an internal control. Transcriptional expression levels of all FPs were normalized and expressed as fold changes with respect to the *gyrA* control. (B) Western blot analysis of FPs expressed in *B. anthracis*. Bacteria were grown as described above and lysed, and equal amounts of protein were subjected to SDS-PAGE and Western blotting using GFP-specific polyclonal antibodies.

and carbon dioxide. For this analysis, we used NBY broth (45), which is a low-nutrient broth shown to promote efficient toxin production in *B. anthracis* (10). Figure 5A shows growth curves and fluorescence over time for both strains and their GFPopt-negative counterparts. High GFPopt expression could be observed only for strain A35 in the presence of carbon dioxide, whereas there was little expression in regulator-negative strains, even in the presence of CO_2. Fluorescence was highest at late exponential and stationary growth phases, showing that the *pagA* promoter is more active during these phases. Western blot analysis of lysates harvested from bacteria at the end of the experiment after approximately 8 h of growth (Fig. 5B) confirms observations made in fluorimetric assays. In comparison to the pXO1-containing strain Ames 35 grown in carbon dioxide, all strains show lower GFPopt expression. These results show the suitability of codon-optimized FPs, in our application GFPopt, for the analysis of promoter activity in *B. anthracis*.

Expression of GFPopt, CFPopt, and YFPopt in *S. aureus*. *S. aureus* is another low-GC-content bacterium for which, to our knowledge, only GFP and YFP have been described as FP reporters (4, 9, 33). Analysis of the original YFP and CFP showed that as in *B. anthracis*, 213 or 226 out of 240 codons can be deemed unfavorable for expression in *S. aureus*. We therefore hypothesized that our newly developed codon-optimized CFPopt and YFPopt proteins might be suitable for expression in *S. aureus*. Initially, we attempted to utilize the *pagA* promoter of *B. anthracis* to control FPopt expression; however, we failed due to its inactivity in *S. aureus* (data not shown), a result which was to be expected. Consequently, we used a previously published tetracycline-inducible promoter that has been shown to function in *S. aureus* (20). We cloned all nonactivatable codon-optimized FPs into plasmid pTetON under the control of the tetracycline-inducible promoter $P_{xyl/tetO}$. This plasmid is a derivative of pYJ335 (20), as outlined in Materials and Methods. Due to lack of tetracycline repressor expression on this plasmid, $P_{xyl/tetO}$ is constitutively active. Ligation of *yfpopt* and *cfpopt* into pTetON and transformation of *S. aureus* RN4220 resulted in high expression of all FPs (Fig. 6). These results demonstrate that our codon-optimized FP genes may be highly suitable as reporter genes not only in *B. anthracis* but also in other low-GC bacteria.

DISCUSSION

FPs have wide applications in imaging bacterial gene expression, promoter activity, and localization of proteins. In comparison to enzymatic reporters, a clear advantage is the ability to monitor gene activity in intact bacteria, a method that stands in contrast to the use of enzymatic reporters, such as β-lactamase or chloramphenicol acetyltransferase, which require lysis of cells and release of the cytosol in order to assess reporter activity. A disadvantage of FPs is that not all bacteria are able to express them at high levels. Here, we were able to show superior expression of two codon-optimized FPs, YFPopt and CFPopt, in the low-genomic-GC-content pathogens *B. anthracis* and *S. aureus*.

Initial sequence comparison between the original FPs and codon-optimized ones with regard to codon usage showed high discrepancies compared to intrinsic *B. anthracis* genes, making them good candidates for codon optimization. By lowering the GC content substantially and adapting the codon usages of fluorescent genes *gfpopt*, *cfpopt*, and *yfpopt* to those preferred

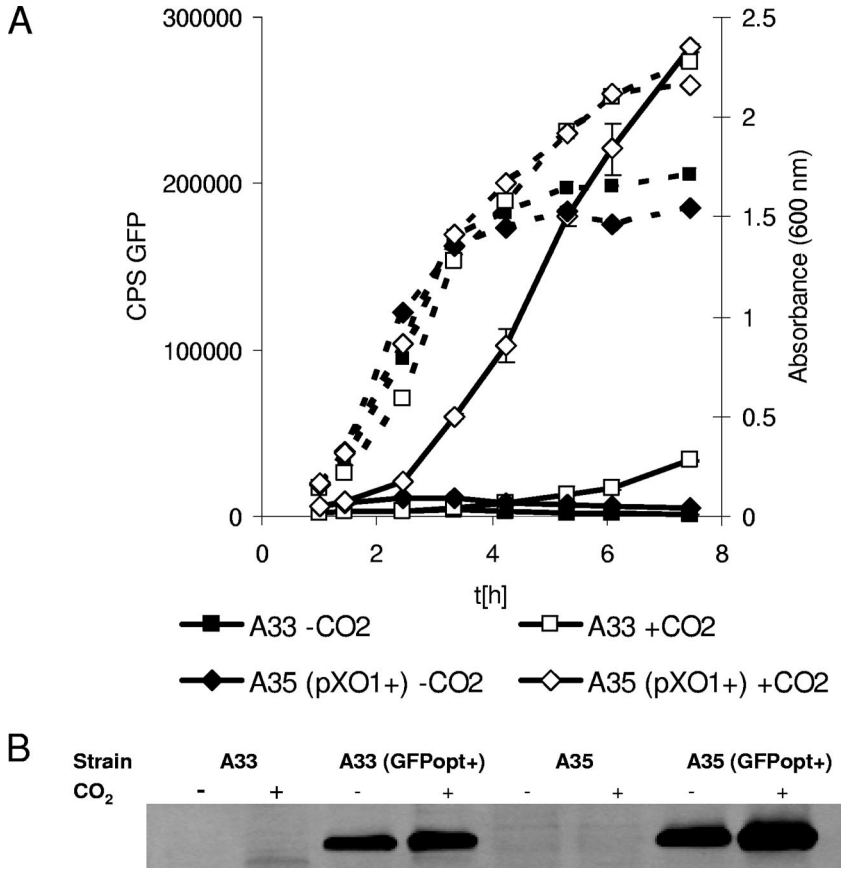

FIG. 5. *pagA* promoter analysis using GFPopt as a reporter. (A) Growth curves (broken lines) and fluorescence intensities (solid lines) of *B. anthracis* expressing GFPopt under the control of the *pagA* promoter. GFPopt-harboring bacteria containing virulence plasmid pXO1 (strain A35) or plasmid free (strain A33) were grown in NBY broth supplemented with 10% FBS in the presence or absence of sodium bicarbonate (0.9%, wt/vol) and a 5% CO_2 atmosphere. At different time points, samples were analyzed for fluorescence in a fluorimeter. CPS, counts per second. Error bars indicate standard deviations. (B) Western blotting of bacteria grown to stationary phase. Lysates were processed as described for Fig. 4.

by *B. anthracis*, we were able to achieve high expression in this bacterium. Strikingly, no expression was observed for the original, nonoptimized genes *cfp* and *yfp*. This phenomenon of better expression after codon optimization has been described previously (3, 27). Surprisingly, although it was not microscopically obvious, we were able to observe differences in fluorescence intensities between the codon-optimized GFPopt and the original GFPmut1 by FACS; the latter was significantly brighter as determined by MFI analysis. We did not expect major differences in the fluorescence of these two proteins, since the GC content and codon utilization are not strikingly dissimilar. Nonetheless, our expectations were to observe a higher fluorescence for the codon-optimized version of the protein. An explanation for this phenomenon might be differential folding and structural properties of the mRNA, since the primary sequence of optimized and nonoptimized *gfp* has been altered, therefore leading to a differential translation rate. Another reason might be better protein folding properties of the original GFPmut1. To further investigate the reasons for expression differences between codon-optimized and original CFPs and YFPs, we performed transcriptional analysis by RT-PCR to quantify mRNA levels. The results showed the presence of all transcripts, with a slightly smaller amount for *cfp* and *yfp*, which could be explained by either mRNA instability or a lower transcription rate; the latter seems unlikely since all FPs were expressed from the same promoter. The fact that mRNAs of genes exhibit different stabilities has been shown for many bacteria and can have multiple reasons, such as secondary structures (hairpins), internal secondary structures marking them for RNase III degradation, or RNase recognition sequences (7). The lower mRNA levels observed for YFP and CFP might explain a lower protein expression but not the total absence of protein that was observed by Western blot analysis. We therefore conclude that a better availability of the cognate tRNAs is the more likely explanation for high expression of CFPopt and YFPopt in comparison to the nonoptimized counterparts.

We were able to demonstrate that our codon-optimized FPs can be used as reporters for promoter activity, as shown by the analysis of the *B. anthracis* PA promoter in response to carbon dioxide, bicarbonate, and the presence of pXO1, the larger virulence plasmid of *B. anthracis* harboring PA regulators AtxA and PagR. The results showed a clear correlation between the presence of CO_2 and promoter activity, measured in GFP fluorescence. Furthermore, the presence of pXO1 greatly influenced PA promoter activity as observed by high fluores-

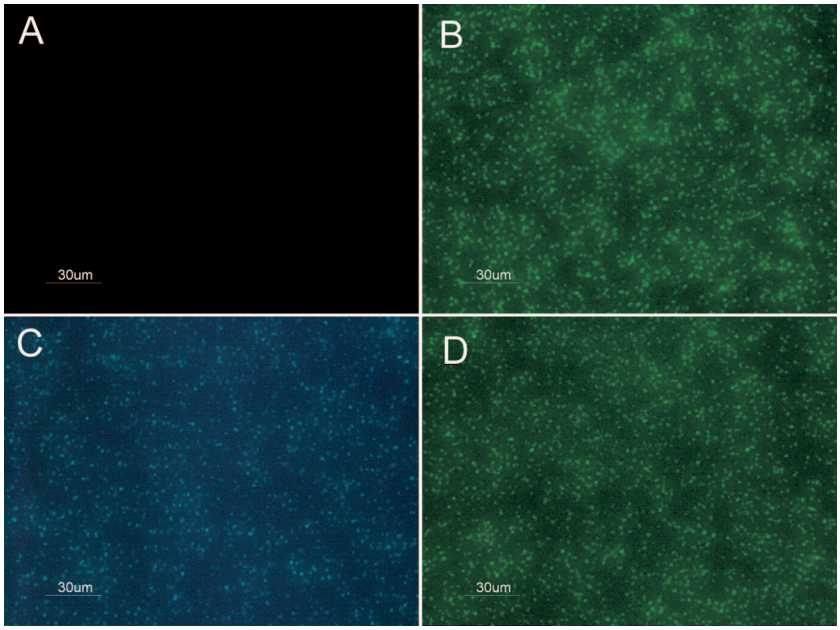

FIG. 6. Fluorescence microscopic analysis of *S. aureus* strain RN4220(pTetON) (A) and RN4220 constitutively expressing GFPopt (B), CFPopt (C), or YFPopt (D) from the $P_{xyl/tetO}$ promoter. Bacteria were grown in tryptic soy broth to stationary phase and microscopically analyzed for fluorescence.

cence, especially during stationary phase. To some degree, the higher fluorescence at later time points could also be caused by accumulation of GFP and amplification of the fluorescent signal within the cells. GFP has been shown to have an extremely long half-life of 24 h or more (25), making it less suitable for promoter reporter activity. Therefore, it would be desirable to have less stable variants for reporter purposes. For some bacteria, such as *Staphylococcus epidermidis* (16) or *Mycobacterium* (5), GFP variants with alternative C termini and substantially shorter half-lives have been described. By varying the C terminus, bacterial proteins can be marked for faster degradation by housekeeping proteases, lowering the half-lives of GFP variants to as low as to 40 min to several hours, depending on the bacterial species (2). Studies to improve our optimized proteins with respect to stability are under way, since the use of a stable FP might prove difficult for true quantitative determination of promoter activities during bacterial growth.

To evaluate whether high expression of our codon-optimized FPs is limited to just *B. anthracis* or whether it could also be applied to other low-GC bacteria, we cloned GFPopt, YFPopt, and CFPopt under the control of a strong promoter for expression in *S. aureus*. Fluorescent microscopic images confirmed that all proteins are also highly expressed in *S. aureus*. Even though YFP has been used to visualize biofilms in *S. aureus* (4), this is to our knowledge the first report showing CFP expression in this bacterium.

We were also able to construct a codon-optimized photoactivatable GFP suited for expression in low-GC bacteria. Photoactivatable proteins find application in mammalian cells, e.g., for monitoring organelle or molecule dynamics within cells (23, 29, 31). By photoactivation, highlighted subpopulations of proteins, organelles, or cells can be monitored temporally, and new synthesis of PAGFP-labeled proteins does not influence observations, as these molecules will not be fluorescent (26). No use of this protein in bacteria has been reported, but applications paralleling those in mammalian cells can be imagined.

Finally, another important observation made was that *B. anthracis* spores derived from bacteria expressing FPs showed high fluorescence which remained stable even after heat inactivation and for a period of at least 14 days. Stable maintenance of GFP within the spore has been reported before (35). These results show that fluorescent spores could be suitable for infection purposes and for monitoring localization of spores within, e.g., mammalian cells; fluorescence intensities of GFP-positive bacteria or spores in host cells may even be used as indicator for multiplicities of infection, as previously shown for *Salmonella* by Thone et al. (44). There are many possible applications for FPs in bacteria; extending the variety of color spectra available for expression in different species of bacteria may help us to understand basic pathogenic mechanisms and expression profiles of virulence factors in vitro and in vivo.

ACKNOWLEDGMENTS

This research was supported by the Intramural Research Program of the National Institute of Allergy and Infectious Diseases, NIH.

We thank Jennifer Chua for assistance with characterization of the PAGFP.

REFERENCES

1. **Abramova, F. A., L. M. Grinberg, O. V. Yampolskaya, and D. H. Walker.** 1993. Pathology of inhalational anthrax in 42 cases from the Sverdlovsk outbreak of 1979. Proc. Natl. Acad. Sci. USA **90:**2291–2294.
2. **Andersen, J. B., C. Sternberg, L. K. Poulsen, S. P. Bjorn, M. Givskov, and S. Molin.** 1998. New unstable variants of green fluorescent protein for studies of transient gene expression in bacteria. Appl. Environ. Microbiol. **64:**2240–2246.
3. **Barrett, J. W., Y. Sun, S. H. Nazarian, T. A. Belsito, C. R. Brunetti, and G.**

McFadden. 2006. Optimization of codon usage of poxvirus genes allows for improved transient expression in mammalian cells. Virus Genes **33:**15–26.
4. **Beyenal, H., C. Yakymyshyn, J. Hyungnak, C. C. Davis, and Z. Lewandowski.** 2004. An optical microsensor to measure fluorescent light intensity in biofilms. J. Microbiol. Methods **58:**367–374.
5. **Blokpoel, M. C., R. O'Toole, M. J. Smeulders, and H. D. Williams.** 2003. Development and application of unstable GFP variants to kinetic studies of mycobacterial gene expression. J. Microbiol. Methods **54:**203–211.
6. **Bradley, K. A., J. Mogridge, M. Mourez, R. J. Collier, and J. A. Young.** 2001. Identification of the cellular receptor for anthrax toxin. Nature **414:**225–229.
7. **Carrier, T. A., and J. D. Keasling.** 1997. Controlling messenger RNA stability in bacteria: strategies for engineering gene expression. Biotechnol. Prog. **13:**699–708.
8. **Chalfie, M., Y. Tu, G. Euskirchen, W. W. Ward, and D. C. Prasher.** 1994. Green fluorescent protein as a marker for gene expression. Science **263:**802–805.
9. **Cheung, A. L., C. C. Nast, and A. S. Bayer.** 1998. Selective activation of *sar* promoters with the use of green fluorescent protein transcriptional fusions as the detection system in the rabbit endocarditis model. Infect. Immun. **66:**5988–5993.
10. **Chitlaru, T., O. Gat, Y. Gozlan, N. Ariel, and A. Shafferman.** 2006. Differential proteomic analysis of the *Bacillus anthracis* secretome: distinct plasmid and chromosome CO_2-dependent cross talk mechanisms modulate extracellular proteolytic activities. J. Bacteriol. **188:**3551–3571.
11. **Cormack, B. P., R. H. Valdivia, and S. Falkow.** 1996. FACS-optimized mutants of the green fluorescent protein (GFP). Gene **173:**33–38.
12. **Dai, Z., J. C. Sirard, M. Mock, and T. M. Koehler.** 1995. The *atxA* gene product activates transcription of the anthrax toxin genes and is essential for virulence. Mol. Microbiol. **16:**1171–1181.
13. **Fairweather, N., S. Kennedy, T. J. Foster, M. Kehoe, and G. Dougan.** 1983. Expression of a cloned *Staphylococcus aureus* alpha-hemolysin determinant in *Bacillus subtilis* and *Staphylococcus aureus*. Infect. Immun. **41:**1112–1117.
14. **Feucht, A., and P. J. Lewis.** 2001. Improved plasmid vectors for the production of multiple fluorescent protein fusions in *Bacillus subtilis*. Gene **264:**289–297.
15. **Fitzgerald, J. R.** 2007. Targeted gene disruption for the analysis of virulence of *Staphylococcus aureus*. Methods Mol. Biol. **391:**103–112.
16. **Franke, G. C., S. Dobinsky, D. Mack, C. J. Wang, I. Sobottka, M. Christner, J. K. Knobloch, M. A. Horstkotte, M. Aepfelbacher, and H. Rohde.** 2007. Expression and functional characterization of gfpmut3.1 and its unstable variants in *Staphylococcus epidermidis*. J. Microbiol. Methods **71:**123–132.
17. **Heim, R., D. C. Prasher, and R. Y. Tsien.** 1994. Wavelength mutations and posttranslational autoxidation of green fluorescent protein. Proc. Natl. Acad. Sci. USA **91:**12501–12504.
18. **Ho, S. N., H. D. Hunt, R. M. Horton, J. K. Pullen, and L. R. Pease.** 1989. Site-directed mutagenesis by overlap extension using the polymerase chain reaction. Gene **77:**51–59.
19. **Hoffmaster, A. R., and T. M. Koehler.** 1999. Autogenous regulation of the *Bacillus anthracis pag* operon. J. Bacteriol. **181:**4485–4492.
20. **Ji, Y., A. Marra, M. Rosenberg, and G. Woodnutt.** 1999. Regulated antisense RNA eliminates alpha-toxin virulence in *Staphylococcus aureus* infection. J. Bacteriol. **181:**6585–6590.
21. **Kamionka, A., R. Bertram, and W. Hillen.** 2005. Tetracycline-dependent conditional gene knockout in *Bacillus subtilis*. Appl. Environ. Microbiol. **71:**728–733.
22. **Kane, J. F.** 1995. Effects of rare codon clusters on high-level expression of heterologous proteins in *Escherichia coli*. Curr. Opin. Biotechnol. **6:**494–500.
23. **Karbowski, M., D. Arnoult, H. Chen, D. C. Chan, C. L. Smith, and R. J. Youle.** 2004. Quantitation of mitochondrial dynamics by photolabeling of individual organelles shows that mitochondrial fusion is blocked during the Bax activation phase of apoptosis. J. Cell Biol. **164:**493–499.
24. **Koehler, T. M., Z. Dai, and M. Kaufman-Yarbray.** 1994. Regulation of the *Bacillus anthracis* protective antigen gene: CO_2 and a *trans*-acting element activate transcription from one of two promoters. J. Bacteriol. **176:**586–595.
25. **Li, X., X. Zhao, Y. Fang, X. Jiang, T. Duong, C. Fan, C. C. Huang, and S. R. Kain.** 1998. Generation of destabilized green fluorescent protein as a transcription reporter. J. Biol. Chem. **273:**34970–34975.
26. **Lippincott-Schwartz, J., and G. H. Patterson.** 2008. Fluorescent proteins for photoactivation experiments. Methods Cell Biol. **85:**45–61.
27. **Mechold, U., C. Gilbert, and V. Ogryzko.** 2005. Codon optimization of the BirA enzyme gene leads to higher expression and an improved efficiency of biotinylation of target proteins in mammalian cells. J. Biotechnol. **116:**245–249.
28. **Muto, A., and S. Osawa.** 1987. The guanine and cytosine content of genomic DNA and bacterial evolution. Proc. Natl. Acad. Sci. USA **84:**166–169.
29. **Palamidessi, A., E. Frittoli, M. Garre, M. Faretta, M. Mione, I. Testa, A. Diaspro, L. Lanzetti, G. Scita, and P. P. Di Fiore.** 2008. Endocytic trafficking of Rac is required for the spatial restriction of signaling in cell migration. Cell **134:**135–147.
30. **Park, S., and S. H. Leppla.** 2000. Optimized production and purification of *Bacillus anthracis* lethal factor. Protein Expr. Purif. **18:**293–302.
31. **Patterson, G. H., and J. Lippincott-Schwartz.** 2002. A photoactivatable GFP for selective photolabeling of proteins and cells. Science **297:**1873–1877.
32. **Pomerantsev, A. P., K. V. Kalnin, M. Osorio, and S. H. Leppla.** 2003. Phosphatidylcholine-specific phospholipase C and sphingomyelinase activities in bacteria of the *Bacillus cereus* group. Infect. Immun. **71:**6591–6606.
33. **Qazi, S. N., E. Counil, J. Morrissey, C. E. Rees, A. Cockayne, K. Winzer, W. C. Chan, P. Williams, and P. J. Hill.** 2001. *agr* expression precedes escape of internalized *Staphylococcus aureus* from the host endosome. Infect. Immun. **69:**7074–7082.
34. **Robinson, M., R. Lilley, S. Little, J. S. Emtage, G. Yarranton, P. Stephens, A. Millican, M. Eaton, and G. Humphreys.** 1984. Codon usage can affect efficiency of translation of genes in *Escherichia coli*. Nucleic Acids Res. **12:**6663–6671.
35. **Ruthel, G., W. J. Ribot, S. Bavari, and T. A. Hoover.** 2004. Time-lapse confocal imaging of development of *Bacillus anthracis* in macrophages. J. Infect. Dis. **189:**1313–1316.
36. **Saile, E., and T. M. Koehler.** 2002. Control of anthrax toxin gene expression by the transition state regulator *abrB*. J. Bacteriol. **184:**370–380.
37. **Schnappinger, D., P. Schubert, K. Pfleiderer, and W. Hillen.** 1998. Determinants of protein-protein recognition by four helix bundles: changing the dimerization specificity of Tet repressor. EMBO J. **17:**535–543.
38. **Scholz, O., A. Thiel, W. Hillen, and M. Niederweis.** 2000. Quantitative analysis of gene expression with an improved green fluorescent protein. Eur. J. Biochem. **267:**1565–1570.
39. **Scobie, H. M., G. J. Rainey, K. A. Bradley, and J. A. Young.** 2003. Human capillary morphogenesis protein 2 functions as an anthrax toxin receptor. Proc. Natl. Acad. Sci. USA **100:**5170–5174.
40. **Siemering, K. R., R. Golbik, R. Sever, and J. Haseloff.** 1996. Mutations that suppress the thermosensitivity of green fluorescent protein. Curr. Biol. **6:**1653–1663.
41. **Skow, A., K. A. Mangold, M. Tajuddin, A. Huntington, B. Fritz, R. B. Thomson, Jr., and K. L. Kaul.** 2005. Species-level identification of staphylococcal isolates by real-time PCR and melt curve analysis. J. Clin. Microbiol. **43:**2876–2880.
42. **Suel, G. M., J. Garcia-Ojalvo, L. M. Liberman, and M. B. Elowitz.** 2006. An excitable gene regulatory circuit induces transient cellular differentiation. Nature **440:**545–550.
43. **Teng, D., Y. Fan, Y. L. Yang, Z. G. Tian, J. Luo, and J. H. Wang.** 2007. Codon optimization of *Bacillus licheniformis* beta-1,3-1,4-glucanase gene and its expression in *Pichia pastoris*. Appl. Microbiol. Biotechnol. **74:**1074–1083.
44. **Thone, F., B. Schwanhausser, D. Becker, M. Ballmaier, and D. Bumann.** 2007. FACS-isolation of *Salmonella*-infected cells with defined bacterial load from mouse spleen. J. Microbiol. Methods **71:**220–224.
45. **Thorne, C. B.** 1968. Transduction in *Bacillus cereus* and *Bacillus anthracis*. Bacteriol. Rev. **32:**358–361.
46. **Tsien, R. Y.** 1998. The green fluorescent protein. Annu. Rev. Biochem. **67:**509–544.
47. **Uchida, I., J. M. Hornung, C. B. Thorne, K. R. Klimpel, and S. H. Leppla.** 1993. Cloning and characterization of a gene whose product is a *trans*-activator of anthrax toxin synthesis. J. Bacteriol. **175:**5329–5338.
48. **Valdivia, R. H., B. P. Cormack, and S. Falkow.** 2006. The uses of green fluorescent protein in prokaryotes. Methods Biochem. Anal. **47:**163–178.
49. **Veening, J. W., W. K. Smits, L. W. Hamoen, J. D. Jongbloed, and O. P. Kuipers.** 2004. Visualization of differential gene expression by improved cyan fluorescent protein and yellow fluorescent protein production in *Bacillus subtilis*. Appl. Environ. Microbiol. **70:**6809–6815.
50. **Yokoe, H., and T. Meyer.** 1996. Spatial dynamics of GFP-tagged proteins investigated by local fluorescence enhancement. Nat. Biotechnol. **14:**1252–1256.
51. **Zhou, J., W. J. Liu, S. W. Peng, X. Y. Sun, and I. Frazer.** 1999. Papillomavirus capsid protein expression level depends on the match between codon usage and tRNA availability. J. Virol. **73:**4972–4982.